Cell, Vol. 108, 233–246, January 25, 2002, Copyright ©2002 by Cell Press

Control of Actin Reorganization by Slingshot, a Family of Phosphatases that Dephosphorylate ADF/Cofilin

Ryusuke Niwa,[1,2] Kyoko Nagata-Ohashi,[3] Masatoshi Takeichi,[4] Kensaku Mizuno,[3] and Tadashi Uemura[1,5,6]

[1] Department of Molecular Genetics
The Institute for Virus Research
Kyoto University
Kyoto 606-8507
Japan

[2] Graduate School of Science

[4] Graduate School of Biostudies
Kyoto University
Kitashirakawa, Sakyo-ku
Kyoto 606-8502
Japan

[3] Department of Biomolecular Science
Graduate School of Life Sciences
Tohoku University
Aoba
Sendai 980-8578
Japan

[5] Core Research for Evolutional Science and Technology (CREST)
Japan Science and Technology Corporation

Summary

The ADF (actin-depolymerizing factor)/cofilin family is a stimulus-responsive mediator of actin dynamics. In contrast to the mechanisms of inactivation of ADF/cofilin by kinases such as LIM-kinase 1 (LIMK1), much less is known about its reactivation through dephosphorylation. Here we report Slingshot (SSH), a family of phosphatases that have the property of F actin binding. In *Drosophila*, loss of *ssh* function dramatically increased levels of both F actin and phospho-cofilin (P cofilin) and disorganized epidermal cell morphogenesis. In mammalian cells, human SSH homologs (hSSHs) suppressed LIMK1-induced actin reorganization. Furthermore, SSH and the hSSHs dephosphorylated P cofilin in cultured cells and in cell-free assays. Our results strongly suggest that the SSH family plays a pivotal role in actin dynamics by reactivating ADF/cofilin in vivo.

Introduction

Regulation of the dynamics of the actin cytoskeleton is fundamental in the construction and remodeling of a variety of polarized subcellular structures. The reorganization of the actin cytoskeleton is controlled at multiple levels. When focused on elongation of actin filaments, profilin promotes the elongation at barbed ends, and capping protein (CP) stabilizes the barbed ends; a member of the ADF (actin-depolymerizing factor)/cofilin family accelerates depolymerization at pointed ends and severs long actin filaments (Carlier et al., 1997; Welch et al., 1997; Borisy and Svitkina, 2000; Chen et al., 2000; Pollard et al., 2000).

Among actin binding proteins, ADF/cofilin is the most-characterized stimulus-responsive mediator of actin dynamics (Moon and Drubin, 1995; Yahara et al., 1996; Theriot, 1997; Bamburg, 1999; Bamburg et al., 1999). In response to insulin and lysophosphatidic acid, LIM-kinases (LIMKs), activated by effectors of Rho family GTPases, phosphorylate ADF/cofilin specifically at Ser-3, and thereby inhibit filament-severing and monomer binding activities of ADF/cofilin proteins (Agnew et al., 1995; Moriyama et al., 1996; Arber et al., 1998; Yang et al., 1998; Maekawa et al., 1999; Sumi et al., 1999; Amano et al., 2001). Testicular protein kinases (TESKs) also phosphorylate Ser-3 of ADF/cofilin and inhibit its activity, although upstream pathways of TESKs activation appear to be separate from that of LIMKs (Toshima et al., 2001a, 2001b, 2001c). ADF/cofilin undergoes rapid dephosphorylation as well in response to several extracellular stimuli, which could result from downregulation of the kinases, upregulation of a phosphatase(s), or both (Moon and Drubin, 1995). In contrast to characterization of the kinases, however, much less is known about the phosphatases that reactivate ADF/cofilin.

Actin dynamics in vivo have been studied genetically in several systems including *Drosophila* (Sutherland and Witke, 1999). Bristles and hairs on appendages are actin-based protrusions exposed on body surfaces; therefore, they are easily scored landmarks for isolating mutations that cause malformations (Overton, 1967; Tilney et al., 1995, 1996, 2000). In fact, loci reported to be involved in such malformations include *chickadee* (*chic*) encoding profilin (Cooley et al., 1992; Verheyen and Cooley, 1994), *cpb* encoding the β subunit of CP (Hopmann et al., 1996), and *twinstar* (*tsr*) encoding ADF/cofilin (Edwards et al., 1994; Gunsalus et al., 1995; Chen et al., 2001). Here we report another locus, which we named *slingshot* (*ssh*) after the bifurcation phenotypes of the bristles and hairs in its mutants. The *ssh* gene encodes a phosphatase that is conserved among several animal species. Loss of *ssh* function dramatically increased the level of actin filaments, which is similar to a phenotype of *tsr* mutant cells (Baum et al., 2000; Baum and Perrimon, 2001). In cultured mammalian cells, such a strong enhancement of actin polymerization is induced by overproduction of LIMKs or TESKs (Arber et al., 1998; Yang et al., 1998; Toshima et al., 2001a, 2001b).

One hypothesis would be that SSH and these kinases share the same substrate, ADF/cofilin, regulate its phosphorylation level, and consequently control its actin-depolymerizing activity. To pursue this possibility, we took multiple approaches. We present evidence here that loss of *ssh* function in *Drosophila* increased the level of phospho-cofilin (P cofilin) and that *ssh* genetically interacted with the *Drosophila* LIMK gene in actin-based cell morphogenesis. In cultured cells, expression of either of two human SSH homologs (hSSHs) with LIMK1 or TESK1 suppressed actin reorganization induced by those kinases; and SSH or hSSHs expression reduced

[6] Correspondence: tuemura@virus.kyoto-u.ac.jp

the level of P cofilin. Finally, SSH and the hSSHs dephosphorylated P cofilin as judged from the results of cell-free assays. Our results suggest that the SSH family plays a critical role in controlling actin dynamics, presumably through dephosphorylating and thus reactivating cofilin in cellular and developmental contexts.

Results

ssh Mutations Caused Malformations of Essentially All Actin-Based Cellular Extensions on Adult *Drosophila* Epidermis

In the course of genetic screening for loci that affect bristle number and/or morphology, we focused on *l(3)01207*, which has one copy of PZ inserted into *CG6238* (Adams et al., 2000; see details in Experimental Procedures). Lethality of *l(3)01207* was due to loss of *CG6238* function, as shown by the facts that the lethality was recovered by remobilization of the P element and by *CG6238* cDNA expression using a widely expressed GAL4 driver, *daughterless* (*da*)-GAL4 (Wodarz et al., 1995). Through subsequent analysis, we found that adult escapers of hypomorphic alleles had bifurcated and twisted bristles (Figure 1). We renamed this locus *slingshot* (*ssh*).

Wing hairs made by *ssh* null cells were much thicker than normal, twisted, and sometimes bifurcated at their tips (Figure 1A). In hypomorphs, hairs were much better shaped; nevertheless, they exhibited the terminal splitting phenotype (Figure 1B). The splitting phenotype was also seen in bristles (Figures 1E and 1F) and lateral branches of the arista, which is the terminal segment of the antenna (Figures 1J and 1K). Closer observation of surfaces of wild-type bristles revealed parallel striation patterns, which are known to reflect alignments of actin bundles underneath pupal cuticles (Figure 1E; Overton, 1967; Tilney et al., 1995, 1996). This pattern was distorted in mutant bristles (Figure 1G). Compound eyes, which were derived from *ssh* clones, showed disorganization of the regular ommatidia pattern and had lost many interommatidial bristles (Figures 1L–1Q).

SSH and Its Human Homologs Are Members of a Phosphatase Family

Our cDNA analysis predicted that *ssh* encodes a protein of 1045 amino acids (Figures 2A and 2B). The SSH protein had a phosphatase domain whose amino acid sequences were distantly related to those of the family of MAP kinase phosphatases (MKPs; Figures 2B and 2C; Keyse, 1995). The protein made from our cDNA construct comigrated with endogenous SSH (Figure 2D), supporting that the cDNA spanned the entire open reading frame. Three human homologs of *ssh* were identified in the draft sequences, and our analysis of transcripts suggested that at least six different polypeptides would be produced from these three loci (Figure 2B). Two of the human proteins (hSSHs), hSSH-1L and hSSH2, were enzymatically active when reacted with an artificial substrate, p-nitrophenyl phosphate (pNPP; Figure 2E). For unknown reasons, we had difficulties in detecting pNPP-hydrolyzing activity of SSH (data not shown); nevertheless, we showed that SSH dephosphorylated P cofilin, which we considered to be a bona fide substrate, as explained later. hSSH3 did not exhibit any activity toward pNPP, and its expression did not reduce the level of P cofilin in COS-7 cells, either.

Besides the catalytic domain, there are two other domains conserved between SSH and hSSHs (domains A and B in Figures 2B and 2C) that did not have known motifs and were unique to the SSH family. Both SSH and hSSH-1L had long C tails of 530 and 609 residues, respectively (Figure 2B), although their sequences were not very similar to each other. We found EST sequences of ascidian, sea urchin, and zebrafish that corresponded to domains A and/or B (AV383773, BG780592, and AI153680, respectively). On the other hand, neither domain A nor B was found in predicted proteins in *Saccharomuces cerevisae*, *Caenorhabditis elegans*, or *Arabidopsis* under standard conditions for searching databases, suggesting that those species may not have *ssh* orthologs. RNA in situ hybridization showed the *ssh* transcripts to be maternally supplied in the embryo and to be expressed broadly in embryonic and imaginal tissues (data not shown).

SSH(wt), But Not SSH(CS), Rescued *ssh* Mutants from Morphological Defects

To assess the importance of the phosphatase activity of SSH during development, we examined whether expression of a catalytically inactive form could rescue the lethality of *ssh* strong mutants and the hair/bristle phenotype in hypomorphs. To design such an inactive form, we followed previous studies on protein tyrosine phosphatases and the MKPs, in which the conserved Cys residue in the catalytic pocket is replaced by Ser (Streuli et al., 1989; Guan et al., 1991; Keyse, 1995; Figure 2C). SSH(wt) expression rescued *ssh* mutants from both the lethality and the hair/bristle phenotype, whereas SSH(CS) did not (Figures 1C, 1D, 1H, and 1I). In wings of the hypomorph examined, 89 hairs out of 392 ($n = 4$) showed the tip splitting; this phenotype was recovered by SSH(wt) expression (2 out of 401; $n = 4$), but not by SSH(CS) expression (101 out of 390; $n = 4$). Subcellular localization of SSH(wt) and that of SSH(CS) were indistinguishable, and both proteins had the ability to bind F actin, as explained later. These results support our view that the catalytic activity of SSH is required for its in vivo roles. In the wild-type background, expression of either SSH(wt) or SSH(CS) by using *da*-GAL4 had no effect on hair/bristle morphogenesis (data not shown).

ssh Function Is Required to Prevent Excessive Actin Polymerization

To study exactly how actin reorganization is affected by *ssh* mutations, we stained *ssh* mutant clones with dye-conjugated phalliodin. Loss of *ssh* function caused a dramatic increase in the level of F actin in a cell-autonomous manner (Figure 3). We found this phenotype in mutant clones in larval imaginal discs (Figures 3A–3F, 3N, and 3O), pupal wings (Figures 3G–3L), and follicle epithelia of the egg chamber (Figure 3M). Along the apico-basal cell axis, overaccumulation of actin filaments was not necessarily restricted to the apical subcellular region; basolateral positions were also brightly stained (Figures 3D–3F). At 30–36 hr after puparium formation (h APF) at 25°C, each epidermal cell in the wing localizes an assembly of actin bundles to its distal-most

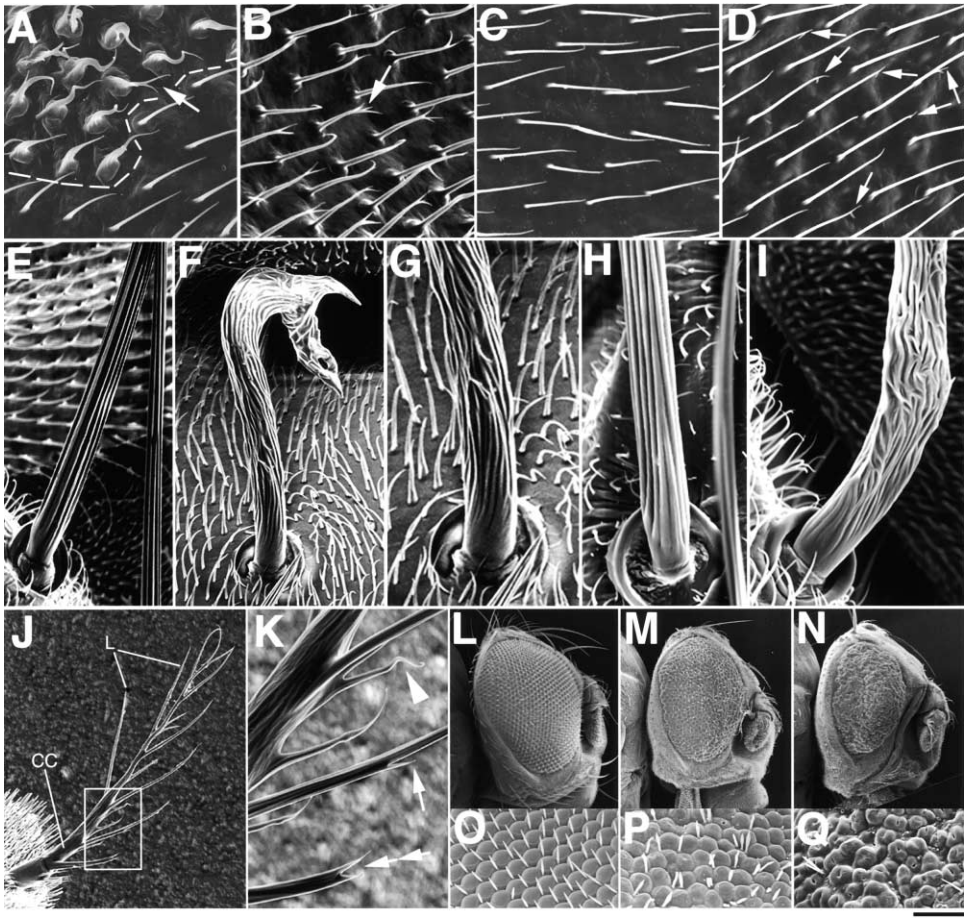

Figure 1. Morphological Defects of Actin-Based Cellular Extensions

(A–D) Wing hairs observed with a scanning electron microscope (SEM).

(A) The broken line indicates a border between a clone (above the line) for a null allele ssh^{1-11} and wild-type cells. Wing hairs made by the *ssh* null cells are much thicker than those of wild-type structures; they are also twisted and often bifurcated at their tips (arrow).

(B) In an adult escaper homozygous for ssh^{51}, wing hairs split near their distal tips (arrow).

(C and D) SSH(wt) expression rescued flies from the splitting phenotype in ssh^{2-4}/ssh^{P01207}, whereas SSH(CS) expression did not (arrows in D).

(E–I) Sensory bristles on the notum. Wild-type straight bristles appear with striation patterns (E). A bristle within a ssh^{1-11} clone was distorted and showed the split-tip phenotype (F) and a disrupted striation pattern ([G], high-power image of [F]). As in (C) and (D), the bristle phenotype was rescued by production of SSH(wt) (H), but not by that of SSH(CS) (I).

(J and K) Arista, a terminal segment of the antenna, in a ssh^{51} homozygote. The arista contains a central core (CC) and a series of lateral side branches (L). These lateral branches are formed from outgrowths of individual core cells (He and Adler, 2001). The boxed area in J is highlighted in K, showing split laterals (arrow), fine abnormal branches (double arrows), and wavy distal tips (arrowhead).

(L–Q) A wild-type eye (L and O) and rough eyes that were made by a ssh^{26-1} clone (M and P) or by a ssh^{P01207} clone (N and Q).

Scale bar equals 7 μm for (A)–(D), 20 μm for (E) and (F), 10 μm for (G)–(I), 70 μm for (J), 17 μm for (K), 200 μm for (L)–(N), and 10 μm for (O)–(Q).

vertex, producing a single prehair in the wild-type (Mitchell et al., 1990). Prehairs of the mutant cells were much more intensely stained with dye-conjugated phalliodin than those of normal cells, indicating that individual mutant hairs contained more actin filaments (Figures 3J–3L). *ssh* null cells seemed to show no obvious defect in proliferation or cell-cell adhesion when compared with cells in wild-type twin spots (see also Figure 1A).

An Increase in the Phosho-Cofilin Level in *ssh* Clones and Genetic Interaction between *ssh* and the *Drosophila* LIM-Kinase Gene

A dramatic increase in the F actin level is also reported in *twinstar* (*tsr*)/*cofilin* clones (Baum et al., 2000; Baum and Perrimon, 2001); in cultured mammalian cells, excessive actin polymerization is caused by overproduction of LIMKs or TESKs (Arber et al., 1998; Yang et al., 1998; Toshima et al., 2001a, 2001b). Therefore, we examined the possibility that those kinases and the SSH family share the same substrate, ADF/cofilin, and thus control the level of phospho-ADF/cofilin in vivo.

We addressed whether loss of *ssh* function increased the level of phosphorylated *Drosophila* cofilin (P Dcofilin) in fly tissues. For this purpose, we first verified binding and specificity of anti-P cofilin antibody, which was originally made against a phosphopeptide of mammalian cofilin (Toshima et al., 2001a), to P Dcofilin (Figures 4A and 4B). When ssh^{1-11} clones were analyzed by staining or Western blotting with this anti-P cofilin antibody, the endogenous P Dcofilin level in *ssh*/*ssh* mutant cells was

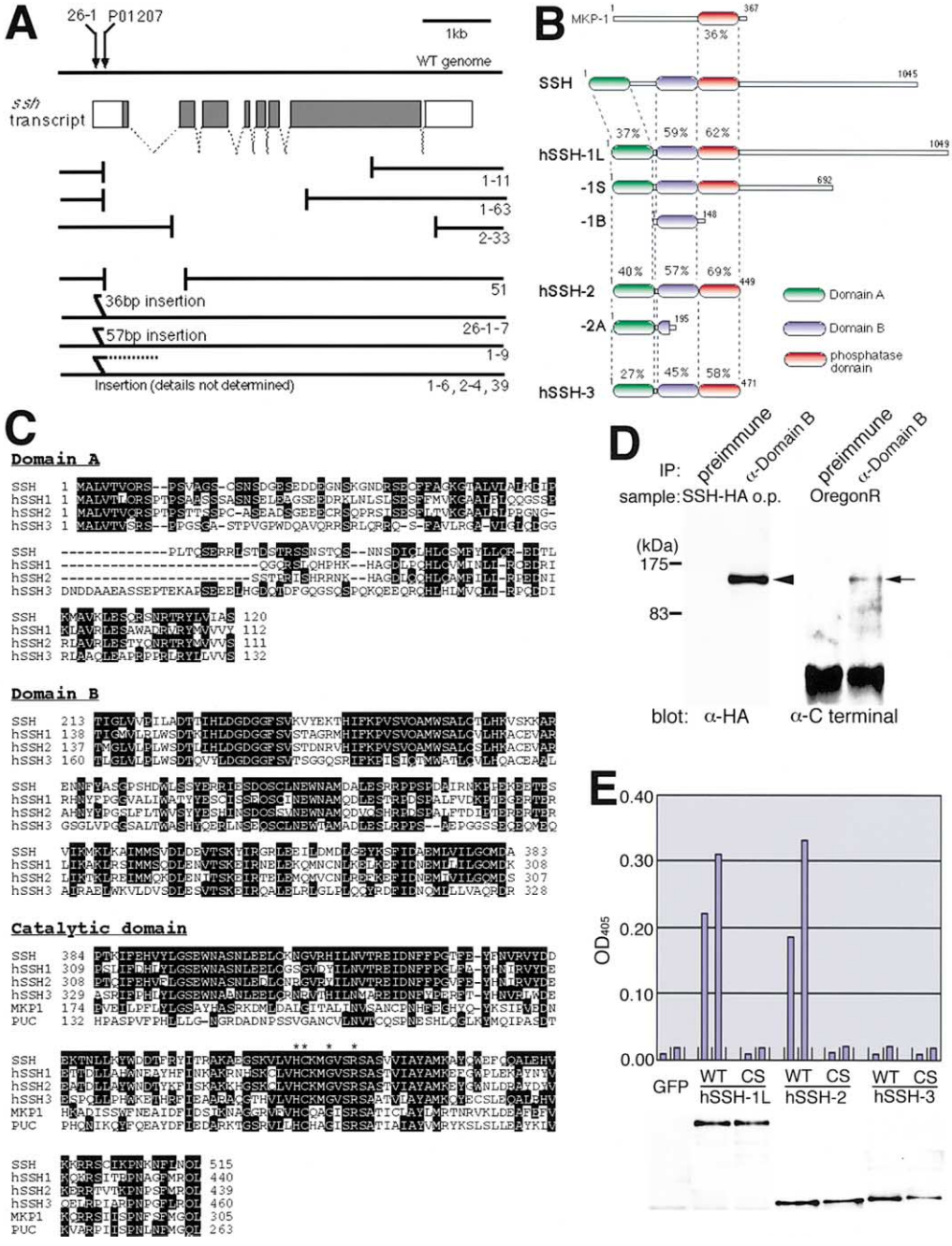

Figure 2. The SSH Family

(A) Exon/intron organization of the *ssh* locus and genomic structures of mutant alleles are illustrated. Closed boxes indicate the open reading frame. Two arrows on the wild-type genome show positions of two independent transposon-insertions, $ssh^{26\text{-}1}$ and ssh^{P01207}, which are 429 bp and 245 bp upstream from the initiation codon, respectively. Deleted genomic regions or lengths of insertions in individual alleles are shown with allele numbers. On the basis of lethal phases and phenotypes either of clones or of escaper adults, we recorded the alleles with decreasing strength in the following series of allele numbers: *1-11*=*1-63*=*2-33*>*P01207*>*26-1*>*51*=*39*>*26-1-7*=*1-9*=*1-6*>*2-4*. The null alleles, $ssh^{1\text{-}11}$, $ssh^{1\text{-}63}$, and $ssh^{2\text{-}33}$ (as homozygotes or heteroallelic heterozygotes) hatched but died at early larval stages, whereas hypomorphic alleles, except for the two P insertion alleles, gave rise to adult escapers.

(B) Schematic representation of predicted polypeptides that are produced from *ssh* and three human genes. Percentages represent amino acid identities between each domain of SSH and that of a human molecule. Also indicated are total numbers of residues of individual proteins.

(C) Multiple alignments of amino acid sequences within each of the three domains. Identical amino acid residues between SSH and the other proteins are shown in black boxes. The catalytic domains of the SSH family share an active site sequence HCxxGxxR (asterisks) of protein tyrosine phosphatases (PTPases) and dual-specificity phosphatases (DSP; Keyse, 1995); also aligned are sequences of two DSPs, human MKP-1/CL100 (NP_004408) and *Drosophila* Puckered (PUC, CAA11282). Consensus sequences of the SSH family are HCKMGVSR, which are unique when compared to those of known PTPases and DSPs. Cys-468 of SSH and equivalent Cys residues in hSSHs were replaced by Ser to construct catalytically inactive forms.

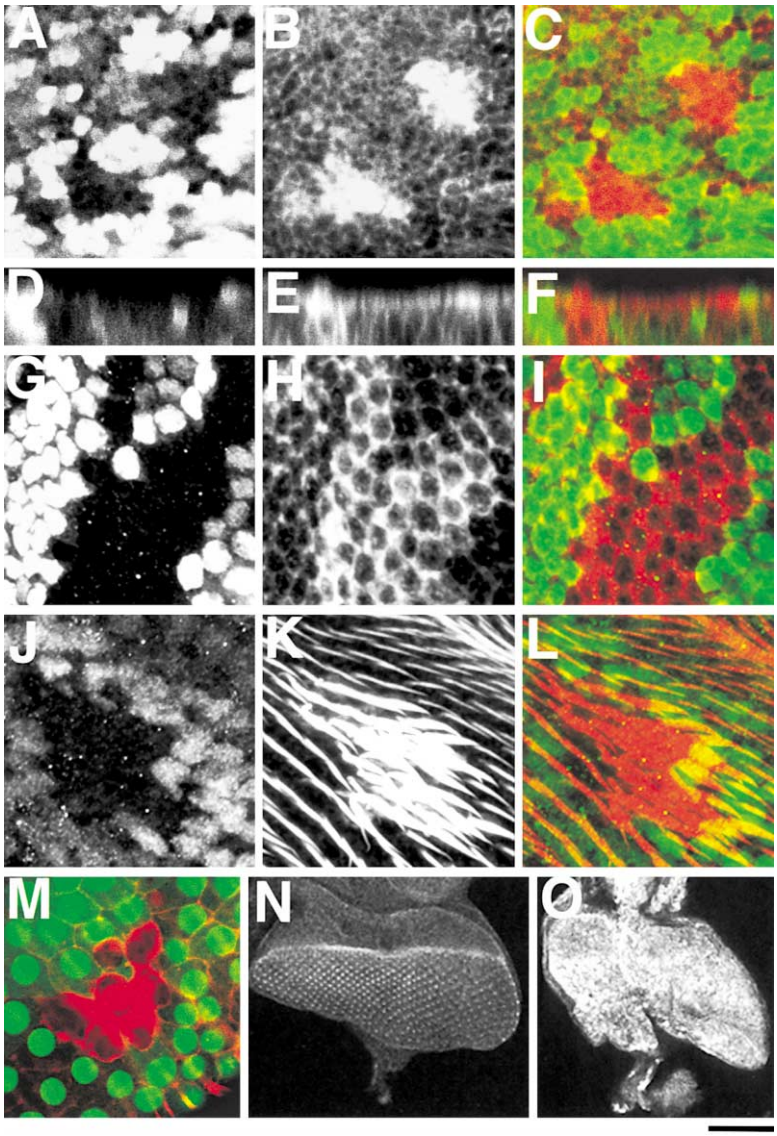

Figure 3. Loss of *ssh* Function Caused a Prominent Increase in the Level of F Actin

(A–M) Clones of cells homozygous for a *ssh* null allele, ssh^{1-11}, were generated by the *Flp-FRT* technique. Tissues were imaged for GFP fluorescence to detect the *ssh* clones (A, D, G, J, and green in M) and for F actin (B, E, H, K, and red in M).

(A–L) Mutant clones in a wing imaginal disc of a third-instar larva (A–F) and in pupal wings [(G–I) 30 hr after puparium formation (h APF); (J–L) 36 h APF]. (D)–(F) are images of vertical sections.

(M) A ssh^{1-11} clone in the follicle epithelium of an egg chamber. (C, F, I, L, and M) Merged images. Clones of *ssh* mutant cells (*ssh*/*ssh*) are recognized by their absence of GFP fluorescence, whereas cells in its twin spot (+/+) have two copies of the GFP marker, and thus they emit stronger fluorescence than *ssh*/+ cells.

(N and O) Phalliodin staining of eye imaginal discs in third-instar larvae.

(N) Wild-type eye disc.

(O) A large ssh^{P01207} clone was made as in Figures 1N and 1Q. Confocal images were collected and processed with identical parameters for (N) and (O).

The scale bar equals 10 μm for (A)–(L), 15 μm for (M), and 80 μm for (N) and (O).

significantly elevated compared with that in the surrounding *ssh*/+ and +/+ wild-type cells (Figures 4D–4F), whereas the total amount of cofilin was not altered (Figure 4C). This result is consistent with the hypothesis that a physiological expression level of SSH is required for dephosphorylating P Dcofilin in vivo.

We also showed genetically that loss of *ssh* function and expression of *Drosophila* LIMK (DLIMK) exerted synergistic effects on wing hair morphogenesis and on the levels of F actin and P Dcofilin (Figures 4G–4O). We first expressed double-stranded RNA (dsRNA) of *ssh* sequences in dorsal cells of the wing, which phenocopied a hypomorphic *ssh* condition through a phenomenon called RNA interference (RNAi; Figure 4J; Kennerdell and Carthew, 2000). DLIMK production of its own, whether the wild-type form (wt) or a kinase-inactive form (KI), did not give detectable phenotypes under the experimental conditions employed (Figures 4G–4I; see details in Experimental Procedures). The weak RNAi phenotype of *ssh* was strongly enhanced by expression of

(D) Detection of endogenous SSH in *Drosophila* embryos. Extracts were made from embryos that overproduced HA-SSH (left) or from wild-type Oregon R embryos (right). Following incubation with either a preimmune serum or an antibody to domain B, immunoprecipitated materials were run in gels and blotted with either anti-HA (left) or anti-C-terminal antibodies (right). A band of 125 kDa was recovered from the wild-type lysate (arrow on the right), which almost comigrated with the tagged protein (arrowhead on the left). The amount of proteins in each lane was equivalent to ~50 μl embryos.

(E) (Top) Wild-type forms (wt) and catalytically inactive forms (CS) of hSSH-1L, hSSH-2, and hSSH-3 were assayed for pNPP-hydrolyzing activity. All forms were (Myc+His) tagged. GFP was a negative control. Reactions were stopped at either 30 min (left bars) or 60 min (right bars). (Bottom) Immunoprecipitates were blotted with an anti-Myc antibody, showing that amounts of wt forms and their CS counterparts were comparable.

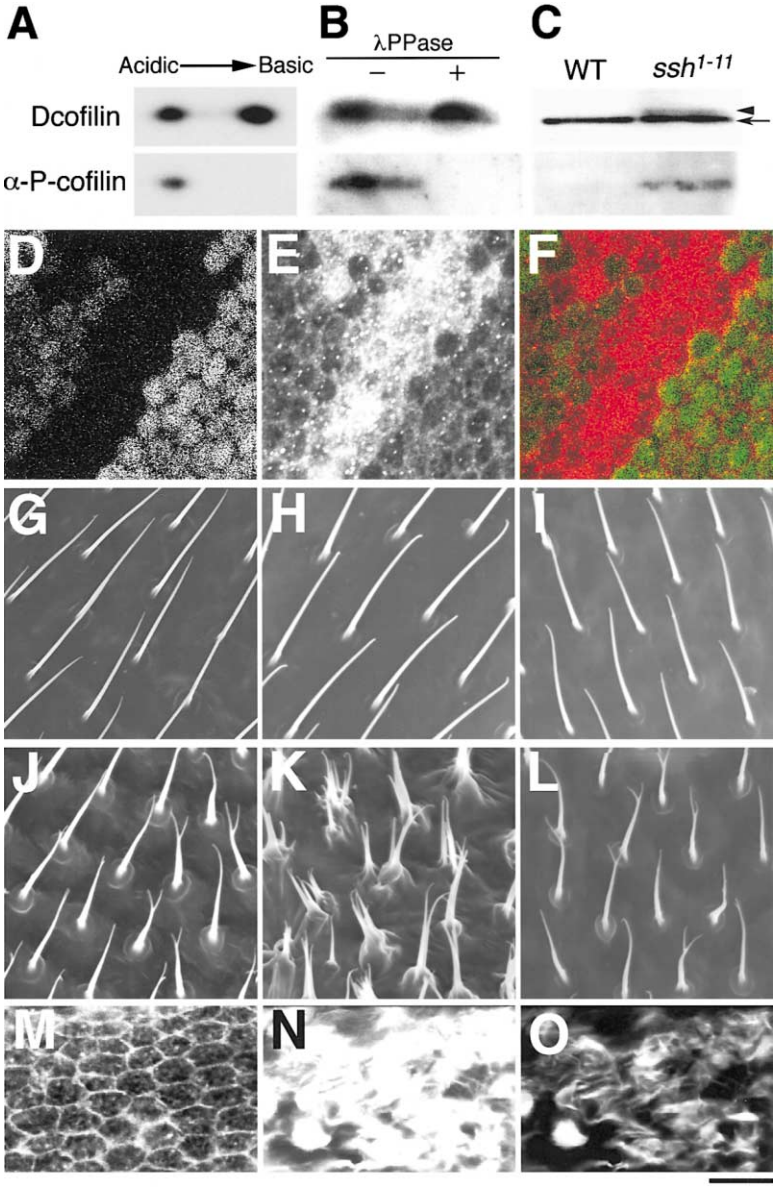

Figure 4. An Increase in the P Cofilin Level in *ssh* Clones and Genetic Interaction between *ssh* and the *Drosophila* LIM-Kinase Gene

(A–C) Western blot analysis of exogenously expressed *Drosophila* cofilin/Twinstar (Dcofilin) in S2 cells (A and B) and endogenous one in eye imaginal discs (C).

(A and B) Binding and specificity of anti-P cofilin antibody to phospho-Dcofilin (P Dcofilin).

(A) His-Dcofilin was expressed in S2 cells, purified, run in two-dimensional gel electrophoresis, and immunoblotted with anti-His antibody (top) and anti-P cofilin antibody (bottom).

(B) The purified Dcofilin was incubated with or without lambda phosphatase and immunoblotted as in (A).

(C) Proteins were extracted from eye discs of the wild-type third instar larva (wt) and those consisting mostly of ssh^{1-11} mutant cells. The total amount of Dcofilin (top) and the P Dcofilin level (bottom) were studied using an antibody to the C-terminal of Dcofilin and anti-P cofilin antibody, respectively. In the lane of the mutant sample, most molecules comigrated with those in wt (arrow); in addition, a slow migrating band was detected faintly (arrowhead). This slow mobility form presumably represents P Dcofilin. *ssh* clones were made as in Figure 3O. The amount of proteins in each lane was equivalent to ten discs.

(D–F) A ssh^{1-11} clone in the pupal wing (30 hr APF) was visualized by loss of GFP fluorescence (D) and stained for P cofilin (E). (F) Merged image.

(G–L) SEM pictures of adult wing hairs. Using *apterous*-GAL4, we expressed the following molecules in the wild-type background: GFP as a negative control (G); *Drosophila* LIMK (DLIMK-wt, [H]); its kinase-inactive form (DLIMK-KI, [I]); hairpin-type double-stranded RNA of *ssh* sequences (*ssh*-dsRNA, [J]); both *ssh*-dsRNA and DLIMK-wt (K); and both *ssh*-dsRNA and DLIMK-KI (L). DLIMK-wt and DLIMK-KI were HA-tagged, and their expression levels were comparable as shown by staining wing discs for the tag (data not shown).

(M–O) Phalloidin staining of pupal wings (30 hr APF) that expressed *ssh*-dsRNA alone (M), and those that coexpressed *ssh*-dsRNA and DLIMK-wt (N and O). Images were collected and processed with identical parameters for (M) and (N); in (O), a much lower gain was set to observe how actin filaments had accumulated. All the crosses were done at 17°C.

The scale bar equals 15 μm for (D)–(F) and (M)–(O) and 4 μm for (G)–(L).

DLIMK-wt (Figure 4K), but DLIMK-KI did not show this enhancement (Figure 4L). Similarly, drastic increases in F actin and P Dcofilin levels resulted from coexpression of the dsRNA and DLIMK-wt (Figures 4M and 4N, data of P Dcofilin not shown). In those cells, unusually thick actin bundles were observed when images were collected with a low gain (Figure 4O). Cells on ventral surfaces were not affected, where the transgene was silent (data not shown).

hSSH Suppressed LIMK1- or TESK1-Induced Actin Reorganization

In addition to experiments using *Drosophila*, we also took the approach of transfecting mammalian cell lines with hSSH plasmids to test the following hypothesis: if hSSH dephosphorylates P cofilin, coexpression of hSSH together with LIMKs or TESKs is expected to counterbalance the promotion effect of those kinases on actin polymerization. To evaluate the degree of actin polymerization, we classified F actin patterns into three categories (Figures 5A–5D, see details in the legend). In control cells expressing GFP alone, strong F actin signals were seen infrequently and most of the cells were scored as class 3 (Figures 5D and 5E), whereas LIMK1 or TESK1 expression made classes 1 and 2 dominant (Figures 5A–5C and 5E). Coexpression of hSSH-1L(wt) or hSSH-2(wt) with either kinase restored class 3 to a dominant category (Figures 5E and 5F–5I); however, the CS forms failed to counteract the kinases (Figures 5E and 5J–5M). These results support that the hSSH phosphatase activ-

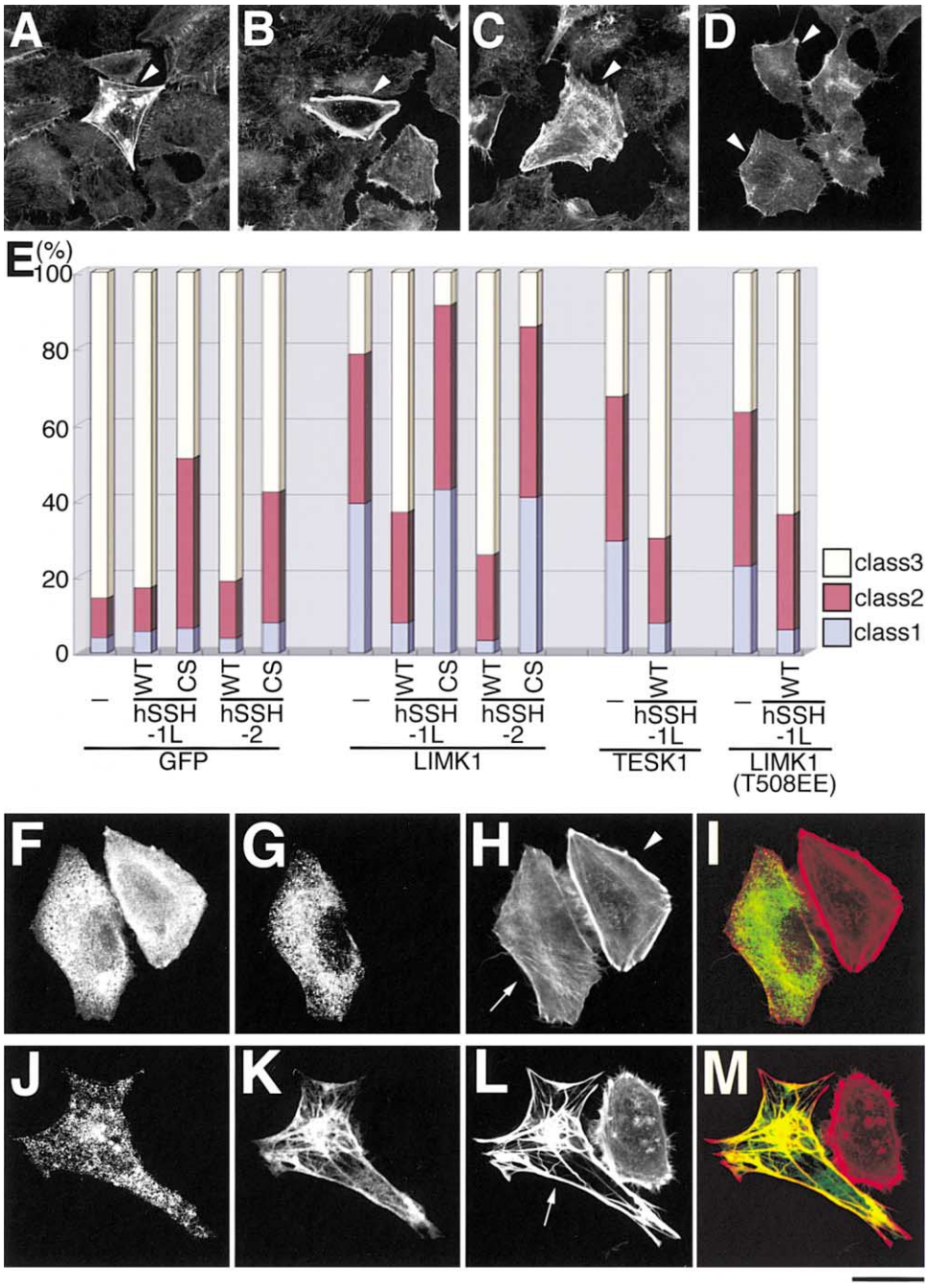

Figure 5. hSSH-1L and hSSH-2 Suppressed LIMK1- or TESK1-Induced Actin Reorganization

(A–D) Classification of patterns of LIMK1- or TESK1-induced actin reorganization. HeLa cells were transfected with a plasmid encoding either HA-tagged LIMK1 or TESK1 and then stained for F actin and the tag. F actin patterns of kinase-expressing cells (arrowheads) fell into three categories: class 1, a punctate appearance (A); class 2, strong signals at the cell periphery and/or in the cytoplasm (B and C); and class 3, no detectable change compared with nontransfected cells (D). (A)–(D) are examples of cells that expressed LIMK1.

(E) Quantitative analysis of F actin patterns. F actin patterns were examined in cells that produced either GFP (a negative control), the kinase (LIMK1 or TESK1), hSSH, or both the kinase and hSSH. LIMK1(T508EE) represents a phosphomimetic form of LIMK1. The images were scored blind by two people, and data of three separate experiments were summed up and displayed ($n > 200$).

(F–M) Cells expressing LIMK1 and hSSH-1L(wt) (F–I), and those expressing LIMK1 and hSSH-1L(CS) (J–M). Cells were stained for HA-LIMK1 (F and J), (Myc+His)-hSSH-1L (G and K), and F actin (H and L). hSSH-1L(wt) expression inhibited actin reorganization induced by LIMK1 (compare arrow and arrowhead in [F]–[I]). In contrast, coexpression of hSSH-1L(CS) and LIMK1 evoked a robust actin reorganization (arrow in [J]–[M]). (I and M) Merged images of hSSH-1L distributions and F actin patterns.

The scale bar equals 30 μm for (A)–(D) and 20 μm for (F)–(M).

ity inhibited LIMK1- or TESK1-dependent actin reorganization.

The above results of the coexpression could be explained by our hypothesis that P cofilin is a direct target of the hSSHs; however, another interpretation is also possible. The kinase activity of LIMK1 is enhanced by phosphorylation at Thr-508 (Ohashi et al., 2000b); therefore, the hSSHs might have dephosphorylated LIMK1 and made it less active. This second hypothesis was less likely because of the result obtained when we used a phosphomimetic form of LIMK1, LIMK1(T508EE). LIMK1(T508EE), which is no longer phosphorylated at the residue of 508, induced actin polymerization; nevertheless, hSSH-1L was still able to counteract LIMK1(T508EE) as it did LIMK1(wt), as shown in Figure 5E.

We found that coexpression of hSSH-1L(CS) with LIMK1 evoked robust assembly of actin filaments in a way that was hardly induced by LIMK1 expression alone (Figures 5J–5M). When compared to F actin patterns in LIMK1-expressing cells (Figures 5A–5C), it looked as if almost all actin filaments in the coexpressing cell were assembled to build a limited number of thick bundles (arrow in Figure 5L). These F-actin patterns were counted as class 2 in Figure 5E. These unusual structures were also induced by expressing hSSH-1L(CS) alone, but not at all by expressing the wild-type form. This abnormal assembly of the filaments was reminiscent of the consequence of coexpression of *ssh*-dsRNA and DLIMK in *Drosophila* epidermal cells (Figure 4K), suggesting the possibility that hSSH-1L(CS) overexpression exerted a dominant-negative effect. hSSH-2(CS) also tended to induce actin reorganization, as shown by a slight expansion of the class 2 population when compared with the effect of its wild-type expression (Figure 5E); however, unlike hSSH-1L(CS), hSSH-2(CS) could not generate the thick actin bundles (data not shown).

hSSH-1L, hSSH-2, and SSH Dephosphorylated P Cofilin in Cultured Cells

A straightforward prediction of the above results would be that expression of hSSH-1L(wt), hSSH-2(wt), or SSH(wt) reduces the P ADF/cofilin level in cells. This was indeed found to be the case (Figures 6A and 6B). Expression of hSSH-1L, hSSH-2, or SSH caused a prominent decrease in the level of P cofilin or P Dcofilin; in contrast, hSSH-3(wt) expression was ineffective. Neither CS forms nor MKP-5, which shows a limited sequence similarity to the catalytic domain of the SSH family, was able to decrease the P cofilin level (Figure 6A). Complementary experiments indicated that hSSH-1L was unable to dephosphorylate p38α and JNK2, which are efficiently inactivated by MKP-5 (Figure 6C; data of JNK2 not shown; Tanoue et al., 1999). These results suggest that the SSH family displays distinct substrate specificity from the MKP family.

Dephosphorylation of P Cofilin by the SSH Family in Cell-Free Systems

Whether hSSH-1L, hSSH-2, and SSH dephosphorylate P cofilin was directly assayed in cell-free systems (Figures 6D–6F). The hSSHs and cofilin were expressed in COS-7 cells; SSH and Dcofilin were expressed in S2 cells. The immunoprecipitated enzymes and the purified substrates, which contained phosphorylated forms, were subject to in vitro reactions. Each wild-type form of the hSSHs or SSH dephosphorylated P cofilin, but the CS forms did not (Figures 6D and 6E), supporting that cofilin is a substrate of hSSH-1L, hSSH-2, and SSH. In our cell-free assay, 90% of P cofilin was dephosphorylated by SSH after 15 min reaction (Figure 6F).

Under our experimental conditions, hSSH-2 was reproducibly less active than hSSH-1L (Figure 6D). When comparable amounts of hSSH-1L(wt) and hSSH-2(wt) were reacted with the same amount of P cofilin, over 99% of the substrate was dephosphorylated by hSSH-1L(wt), whereas only 60% was by hSSH-2(wt). ADF (also called destrin) is a close relative of cofilin in the vertebrate ADF/cofilin family and is also phosphorylated at Ser-3 by LIMKs and TESKs (Amano et al., 2001; Toshima et al., 2001a); we showed that hSSH-1L dephosphorylated phospho-ADF as well (Figure 6G).

We attempted to exclude the possibility that cofilin, isolated from cultured cells, was contaminated by some endogenous phosphatase that is unrelated to the SSH family. For this purpose, we prepared cofilin that had been made in *E. coli* and ^{32}P-labeled by LIMK1 as a substrate. Dephosphorylation reactions were monitored by autoradiography, and we confirmed the enzymatic activity of hSSH-1L toward ^{32}P-labeled cofilin (Figure 6H).

Ser/Thr phosphatases PP1 and PP2A were shown to dephosphorylate P cofilin in vitro (Ambach et al., 2000); therefore, we compared pharmacological features of hSSH-1L, hSSH-2, and SSH with those of PP1 and PP2A (Figures 6D and 6E). The activities of the SSH family members were not inhibited in the presence of 1 μM okadaic acid or 1 μM calyculin A, each of which inhibited PP1 and PP2A almost completely, as previously established (Cohen, 1990). Sodium vanadate has a broad specificity toward tyrosine and dual-specific phosphatases, and a 1 mM concentration of it blocked the activities of the SSH members.

F Actin Binding Property of the SSH Family

In our transfection experiment in Figure 5, we found that hSSH-1L(CS) were predominantly colocalized with F actin (Figures 5K–5M). This result prompted us to investigate whether hSSHs and SSH had the property of binding F actin. Tagged hSSHs and SSH were incubated with actin filaments and centrifuged to examine whether each of them cosedimented with F actin or not (Figure 7A). Both wild-type and CS forms of hSSH-1L and SSH preferentially cosedimented with actin filaments, whereas hSSH-2(wt), hSSH-2(CS), and hSSH-3(wt) exhibited weaker binding capabilities. A fraction of hSSH-3(CS) precipitated in the absence of actin filaments; thus, whether hSSH-3(CS) binds F actin or not was difficult to address with this method. Consistent with the result of the cosedimentation assay, SSH(wt) and SSH(CS) appeared to colocalize with cortical actin in wing epithelia at 30 h APF (Figures 7B–7D, data of SSH(CS) not shown).

Discussion

SSH, hSSH-1L, and hSSH-2 Are Most Likely Cofilin Phosphatases

Drosophila Slingshot (SSH) belongs to a family of phosphatases. Our studies using the whole animal and cell

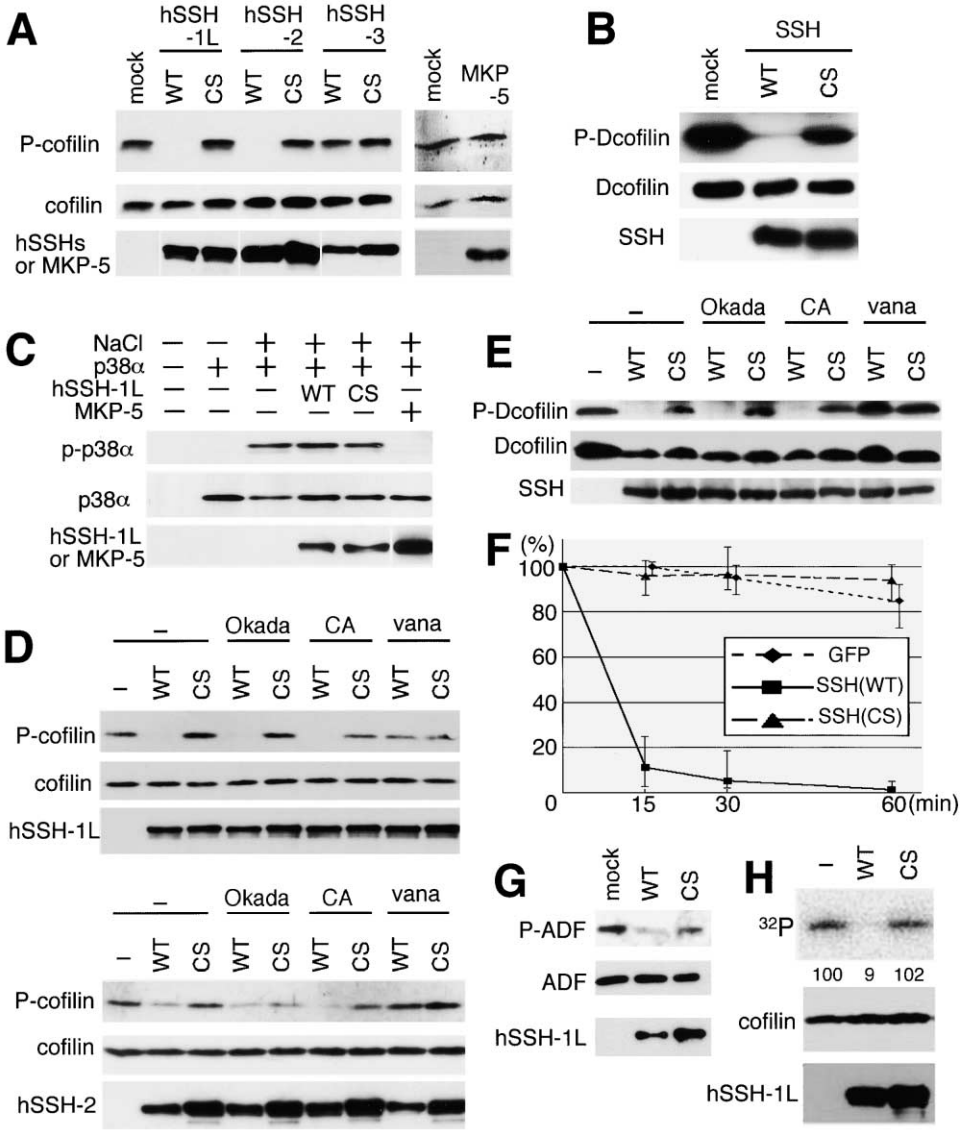

Figure 6. hSSH-1, hSSH-2, and SSH Dephosphorylated P Cofilin in Cells and in Cell-Free Assays

(A–C) Cell transfection experiments.

(A and B) hSSH or SSH expression reduced the level of P cofilin in COS7 or S2 cells.

(A) COS7 cells were transfected with a plasmid encoding one of (Myc+His)-hSSH forms or 3xMyc-MKP-5. The cells were lysed and analyzed by immunoblotting for P cofilin, both phospho- and nonphospho-cofilin, and hSSHs or MKP-5.

(B) His-Dcofilin was expressed in S2 cells with or without HA-SSH. Dcofilin was precipitated and analyzed by immunoblotting to detect P Dcofilin and Dcofilin. Aliquots of the cell lysates were blotted to monitor SSH expression.

(C) COS7 cells were transfected with HA-p38α with or without hSSH-1L or MKP-5 and then stimulated by 0.5 M NaCl for 20 min to activate p38α. Cell lysates were immunoblotted to detect phospho-p38α (p-p38α), p38α, and hSSH-1L or MKP-5. MKP-5 dephosphorylated p38α, but hSSH-1L did not.

(D–H) Cell-free assays to monitor dephosphorylation of P cofilin or phospho-ADF (P ADF).

(D) Purified His-cofilin was reacted with the immunoprecipitated (Myc+His)-hSSH and then analyzed with anti-P cofilin antibody and with anti-His antibody to confirm comparable amounts of cofilin and hSSH in the reactions. Reactions were performed in the presence or absence of each of the following phosphatase inhibitors: okadaic acid (okada, 1 μM), calyculin A (CA, 1 μM), and sodium vanadate (vana, 1 mM).

(E) Purified His-Dcofilin was reacted with HA-SSH, and the reactions were analyzed essentially as in (D).

(F) The purified Dcofilin was incubated with SSH(wt), SSH(CS), or GFP for the indicated minutes and analyzed as in (E). The band intensity was measured, and the ratio of P Dcofilin to the total amount of Dcofilin was plotted against the reaction time, with the ratio at zero time taken as 100%.

(G) Purified His-ADF was reacted with hSSH-1L, and its dephosphorylation was monitored with anti-P cofilin antibody, which also binds to P ADF (Toshima et al., 2001a).

(H) Recombinant His-cofilin, which was made in *E. coli* and phosphorylated by LIMK1 in vitro, was reacted with hSSH-1L and then analyzed by autoradiography (top) and immunoblotting (bottom). In the autoradiograph are indicated relative values of [^{32}P]cofilin band intensity with the level in the reaction without hSSH-1L taken as 100.

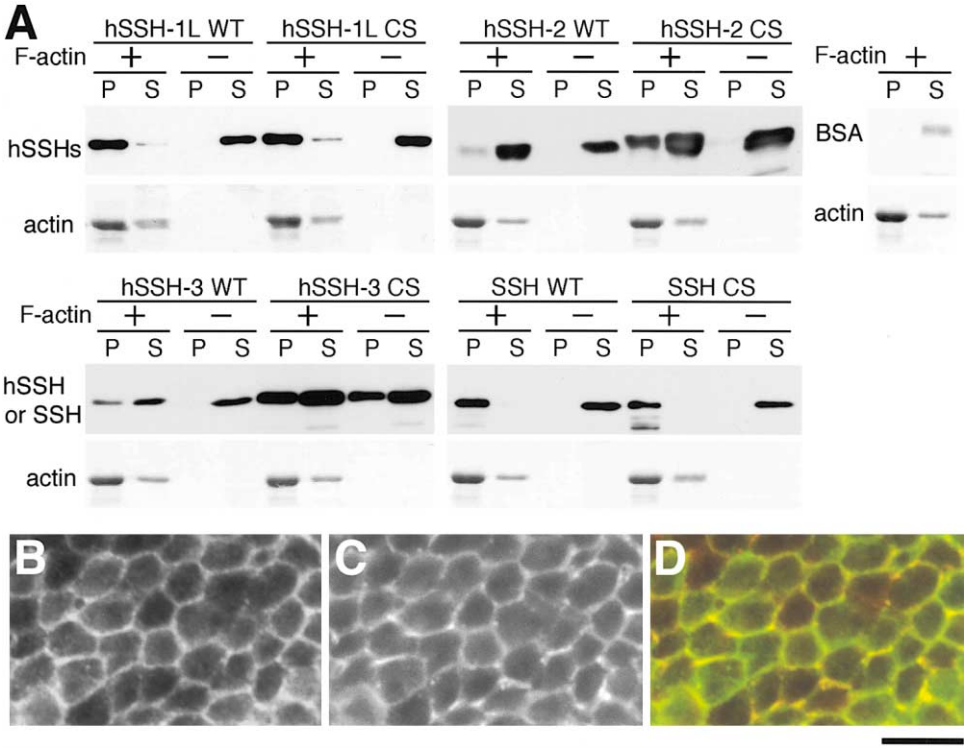

Figure 7. Actin Binding Properties of hSSHs and SSH

(A) (Myc+His)-hSSHs and -SSH, which were expressed in COS-7 cells, were incubated with actin filaments and centrifuged to study whether each SSH family member cosedimented with F actin or not. Abbreviations are as follows: P, pellet; S, supernatant; + and − indicate whether individual SSH family member was incubated with or without F actin, respectively. Actin was visualized by amido black staining. BSA did not coprecipitated with F actin (a negative control).

(B–D) HA-SSH(wt) was expressed by using *sca*-GAL4. Pupae were fixed at 30 hr APF and stained for the HA tag (B) and F actin (C). (D) Merged image. The scale bar equals 10 μm (B–D).

lines demonstrated that SSH and two human homologs (hSSH-1L and -2) prevented excessive actin polymerization and that those SSH family members reduced the P cofilin level in cells. We also showed in cell-free assays that SSH and the hSSHs possessed the activities of dephosphorylating cofilin efficiently and binding to actin filaments. All of our results are consistent with the hypothesis that SSH and the hSSHs control reorganization of actin cytoskeleton by reactivating cofilin. Both the cofilin-phosphatase activity and the F actin binding ability of hSSH-2 were weaker than those of hSSH-1L under our experimental conditions. Extensive domain-swapping between hSSH-1L and -2 may answer if the two activities are related to each other.

In most of our cell-free assays, we prepared the substrate and the SSH-family members by expressing tagged molecules in cultured cells and subsequent precipitation. It might be a concern that our preparations were contaminated by an endogenous phosphatase that is unrelated to the SSH family. We consider the possibility that the substrate was contaminated unlikely for the following reasons. First, the cofilin phosphatase activity was detected when we exogenously added immunoprecipitates of the wild-type forms of the SSH family, but not when we added those of the CS mutants. Second, although PP1 and PP2A are reported to form physical complexes with cofilin in T lymphoma cell lines (Ambach et al., 2000), the activities we detected were resistant to a dose of okadaic acid or calyculin A that almost totally inhibits PP1 and PP2A. Finally, we prepared cofilin, which was made in *E. coli* and phosphorylated by LIMK1 in vitro, and reproduced the phosphatase activity. It is difficult to completely rule out that the in vitro activities we measured were derived from some other phosphatases that were coimmunoprecipitated with SSH or hSSHs. However, if such enzymes should exist, they would associate only with the wild-type forms and not with the CS forms; alternatively, those coprecipitated enzymes would be dephosphorylated and activated by the wild-type SSH or hSSHs.

In genomes of *S. cerevisiae*, *C. elegans*, and *Arabidopsis*, we have found no ortholog of LIMK, TESK, and SSH encoded, although cofilin in any of these species has a Ser-3 or equivalent serine residue. This is suggestive of a model in which the actin-depolymerizing activity of cofilin in those species may be regulated in vivo by a set of enzymes structurally distinct from LIMK, TESK, and SSH. Alternatively, the activity may not be regulated by the serine phosphorylation, but by other means such as PIP2 binding or intracellular pH changes. The latter possibility is supported in *S. cerevisiae* and *D. discoideum* by the report that P cofilin was not detected in vegetatively growing cells (Yahara et al., 1996).

Roles of SSH in Epithelial Cells

Our analysis on *ssh* mutants showed that a critical role of SSH is in building wing hair, bristle, and arista, presumably through reactivating P cofilin. These cellular

extensions in insects share a number of structural features with those found throughout the animal kingdom, such as the brush border of intestinal epithelial cell (Bartles, 2000; DeRosier and Tilney, 2000). Formation of all those protrusions on apical cell surfaces requires packing of parallel filaments through actin-bundling proteins. Therefore, thickening and/or splitting phenotypes in *ssh* mutants are most likely due to overaccumulated filaments that were not arranged in a normal array. SSH did not appear to be required for cell proliferation or viability, which provides a contrast to an effect of loss of a generic enzyme PP1 or PP2A (Axton et al., 1990; Wassarman et al., 1996). All these results are consistent with our hypothesis that cofilin is the major substrate of SSH and that SSH does not display broad substrate specificity.

It is worth noting that mutations of some other loci caused phenotypes similar to or reminiscent of those of *ssh* and *twinstar* (*tsr*)/*cofilin*. In *act up* (*acu*)/*caplet* (*capt*) clones in imaginal discs and follicle cells, the level of actin filaments is elevated as in *ssh* clones, and bristle malformation is described (Baum et al., 2000; Benlali et al., 2000). *acu*/*capt* encodes cyclase-associated protein (CAP), and CAP limits filament formation catalyzed by Ena at apical cell junctions (Baum and Perrimon, 2001). The splitting or branching of wing hair, bristle, and arista is caused by loss of *tricornered* (*trc*) or *furry* (*fry*) (Geng et al., 2000; Cong et al., 2001). The TRC protein is an evolutionally conserved kinase; FRY is also conserved among species, but its biochemical function is unknown. It would be intriguing to explore whether *trc* or *fry* phenotypes are associated with altered levels of actin filaments and P cofilin.

Our current studies did not focus on pursuing whether or not SSH regulates cofilin functions in cell behaviors other than epithelial cell morphogenesis. For example, one of important functions of ADF/cofilin is the dynamic regulation of the cortical ring at the cleavage furrow to complete cytokinesis (Nagaoka et al., 1995; Abe et al., 1996). During ana/telophase in *tsr* mutants, aberrantly large actin-based structures appear at the site of contractile ring formation and fail to disassemble at the end of telophase (Gunsalus et al., 1995). The apparent dispensability of SSH in mitosis in the wing could be explained by the possibility that only a small fraction of active cofilin molecules are required for dynamics of the contractile ring and/or that a cofilin-phosphatase(s) other than SSH is responsible for the progression of cytokinesis.

Is the SSH Family Involved in Stimuli-Driven Actin Reorganization?

In response to extracellular stimuli, some cells are known to undergo rapid dephosphorylation of ADF/cofilin (Moon and Drubin, 1995); all of these stimuli result in cytoskeletal reorganization, possibly by way of reactivation of ADF/cofilin. During semaphorin-3A (Sema-3A)-induced growth cone collapse, a rapid increase and subsequent decrease in P cofilin occurred in growth cones within 5 min after exposure to Sema-3A (Aizawa et al., 2001). This supports a mechanism of local and transient regulation of phosphorylation-dephosphorylation cycling. In some systems, stimulation of cortical actin dynamics occurs without a net change in the ratio of P to non-P ADF/cofilin. Instead, what may be crucial is the turnover rate of the P ADF/cofilin pools or differential distributions of phosphorylation and dephosphorylation spots within cells (Meberg et al., 1998; Yang et al., 1998). Our studies raise an obvious question to be addressed, that is, whether the SSH family is involved in the above stimuli-driven actin reorganizations. It is thus necessary to explore whether the activity of the SSH family is regulated in response to the stimuli, and if so, to determine the components of such regulatory mechanisms.

Experimental Procedures

Molecular Cloning

Full-length *ssh* cDNA (GenBank accession number AB036834) was constructed by screening embryonic cDNA libraries by using LD17262 (Rubin et al., 2000; purchased from Genome Systems) as a probe, and also by 5′-RACE-PCR, using embryonic cDNA as a template. Transcripts of 4.5 kb were detected in embryonic poly(A)$^+$-RNA by Northern blot analysis. To inactivate *ssh* by RNAi (Kennerdell and Carthew, 2000), we designed a hairpin-type double-stranded RNA (dsRNA), in which 0.7 kb antisense and sense strands (nucleotides 623–1353) were connected by 0.7 kb GFP sequences. For expression in *Drosophila* and S2 cells, inserted into pUAST (Brand and Perrimon, 1993) were cDNA for HA-SSH(wt) or SSH(CS), the *ssh*-dsRNA construct, HA-tagged *Drosophila* LIM-kinase cDNA (Ohashi et al., 2000a), and $(His)_6$-*Drosophila* cofilin cDNA (Ohashi et al., 2000a). Exon/intron organization of *ssh* was determined by comparing cDNA and genomic sequences of our own as well as those of the Berkeley *Drosophila* Genome Project (BDGP; Adams et al., 2000). Genomic organization of *ssh* alleles was characterized by PCR using a pair of primers (nucleotides 8–31 and 4220–4242). A plasmid of *UAS-GFP.RN3* was previously described (Usui et al., 1999).

Human *ssh* homologs were identified in the draft sequence of BAC clones, NT_009660 (chromosome 12), NT_010808 (chromosome 17), and NT_008940 (chromosome 11). Open reading frames were predicted on the basis of sequences of RACE-PCR-amplified cDNA clones and of the following EST clones (purchased from Research Genetics): BG479594 and BG397630 for hSSH-1L and -1S, respectively; AA344694 for hSSH-1B; AI272231 for hSSH-2; AW247270 for hSSH-2A; and AA368162 for hSSH-3. Using the expression vector pcDNA3.1/Myc-His(+) (Invitrogen), we made constructs of (Myc+His)-tagged versions of hSSH-1L, hSSH-2, hSSH3, and SSH. Plasmids coding for mammalian cofilin/ADF and the kinases are as follows: mouse cofilin (Moriyama et al., 1996), human ADF (Toshima et al., 2001a), rat TESK1 (Toshima et al., 1999), human LIMK1 (Ohashi et al., 2000b), and LIMK1(T508EE) (Ohashi et al., 2000b). Plasmids used to express Myc-MKP-5 and HA-p38α were as described (Tanoue et al., 1999). GenBank accession numbers for nucleotide sequences of cDNA clones are AB072355 (hSSH-1L), AB072356 (hSSH-1S), AB072357 (hSSH-1B), AB072358 (hSSH-2), AB072359 (hSSH-2A), and AB072360 (hSSH-3).

Drosophila Strains

Baculovirus p35 is an inhibitor of caspases and its expression in *Drosophila* suppresses apoptosis (Hay et al., 1994). p35 expression in wing discs increased the number of bristles in the scutellum, and those supernumerary bristles were often malformed. In our search for genetic modifiers of this p35-induced phenotype, we isolated *l(3)01207*, which had been generated by the BDGP (Spradling et al., 1995, 1999) and has one copy of PZ inserted into *ssh* at band 96B of the third chromosome. *l(3)01207* was provided by the Bloomington Stock Center, and it was cleaned up by crossing *ry* through five generations to segregate out background mutations. As a result, it turned out that the modifier was not linked to the PZ insertion. We renamed this PZ-insertion allele ssh^{P01207}. One of our p[*UAS-ssh*] transgenic lines did not complement the lethality of ssh^{P01207}, indicating that the transgene was inserted into the *ssh* locus in that line; it was designated as $ssh^{26\text{-}1}$. By remobilizing each transposon by Δ2-3 (Robertson et al., 1988), precise and imprecise jumpers were made from $ssh^{P01207}$and $ssh^{26\text{-}1}$.

Transgenes were expressed by using the GAL4-UAS system

(Brand and Perrimon, 1993), such as *apterous* (*ap*)-GAL4 (Lu et al., 1999), *daughterless* (*da*)-GAL4 (Wodarz et al., 1995), and *scabrous* (*sca*)-GAL4 (Klaes et al., 1994). *Drosophila* embryos of OregonR and p[*da-Gal4*]/p[*UAS-ssh*] were homogenized in TBS containing 1% NP-40 and 1% Triton X-100 and used for immunoprecipitating endogenous and overproduced SSH, respectively. Lethality and visible phenotypes were rescued in animals of p[*da-Gal4*] $ssh^{26\text{-}1}$/p[*UAS-ssh*] ssh^{P01207} and p[*da-Gal4*] $ssh^{2\text{-}4}$/p[*UAS-ssh*] ssh^{P01207}, respectively. *ssh* clones were made with the *Flp-FRT* system. Relevant genotypes were *hsp-70-flp*/+; p[*FRT*]82B *ssh*/p[*FRT*]82B p[*hs-GFP*] (Xu and Rubin, 1993; Jiang and Struhl, 1998) and *eyFLP*/+; p[*FRT*]82B *ssh*/p[*FRT*]82B *Minute* (Newsome et al., 2000). *Drosophila* was usually grown at 25°C except for crosses to express DLIMK (Figure 4), which were done at 17°C. DLIMK(wt) expression using *ap*-GAL4 caused lethality at 25°C.

Transfection of Cultured Cells

HeLa, COS-7, and S2 cells were transfected with plasmids by using Effectene Transfection Reagent (Qiagen) or LipofectAMINE2000 reagent (Lifetech) according to the manufacturer's instructions. *Drosophila* cofilin and SSH were expressed in S2 cells by cotransfecting the cells with *actin5C-Gal4* (a gift from Yasushi Hiromi) and the appropriate pUAST construct. Cells were either fixed for staining at 36 hr or solubilized at 48 hr after transfection.

Phosphatase Assays

Cell lysates were made in lysis buffer consisting of 50 mM HEPES (pH 7.4), 2 mM EGTA, 2 mM $MgCl_2$, 1% NP-40, 1% Triton X-100, 10% glycerol, and Complete-mini EDTA-free (Roche Diagnostics). His-cofilin was purified through binding to Ni-NTA agarose (Qiagen) and subsequent elution with imidazole elution buffer (500 mM imidazole [pH 7.5], 1 mM DTT, and 0.1 mg/ml BSA). HA-SSH and (Myc+His)-hSSH were precipitated by using anti-HA (Y-11, Santa Cruz) and anti-Myc (9E10, Santa Cruz) or Ni-NTA agarose, respectively, and suspended in dephosphorylation reaction buffer (50 mM imidazole [pH 7.5] for SSH or 50 mM HEPES [pH 7.4] for hSSH, both containing 1 mM DTT, and 0.1 mg/ml BSA).

Each reaction mixture in Figures 6D and 6G consisted of ~1/5–1/3 of the total hSSH precipitate prepared from COS-7 cells in a 100 mm dish and 1/100 of mouse cofilin or human ADF produced on the same culture scale. Each reaction in Figure 6E included 1/2 of the total SSH immunoprecipitate from S2 cells in a 60 mm dish and 1/10 of the total *Drosophila* cofilin produced on the same culture scale. Each reaction was performed in 30 μl at 25°C for SSH or at 30°C for hSSH for 2 hr except for those in Figure 6F. ^{32}P-labeled cofilin, used in Figure 6H, was prepared as previously reported (Toshima et al., 2001a) and reacted with the hSSH precipitate; the radioactivity was measured using BAS1800 Bio-image Analyzer (Fuji Film). The purified Dcofilin was reacted with or without 200 units of lambda protein phosphatase (NEB) in a buffer supplied by the manufacturer. Okadaic acid and Calyculin A were purchased from Calbiochem and Sigma, respectively.

For measurement of the pNPP-hydrolyzing activity of individual molecules (Figure 2E), each immunoprecipitate obtained with anti-Myc was suspended in 200 μl of 25 mM sodium acetate (pH 5.0), 10 mM pNPP, 1 mM DTT, and 20% glycerol. Reactions were performed at 30°C for 30 min or 60 min and stopped by adding NaOH; pNPP hydrolyzed was measured by absorbance at 405 nm with a microplate reader (Wallac).

Antibodies and Western Blot Analysis

Antibodies to SSH were rabbit antisera against a synthetic peptide (residues 276–295 within domain B) and rat antisera to a fusion protein containing the C terminus (residues 586–1045). Anti-Dcofilin/Twinstar antibody was raised against a C-terminal peptide CREAVE EKLRATDRQ. To monitor the level of phospho-cofilin (P cofilin) or -ADF in COS-7 cells, we solubilized hSSH-expressing cells in the lysis buffer described in "Phosphatase Assays" and placed the lysates on ice for 30 min. Then, the lysates were boiled in the sample solution for SDS-PAGE, separated on 7.5% or 15% gels, and transferred to PVDF (for blotting cofilin or ADF) or nitrocellulose membrane. Typically, a 1 ml lysate was made from COS-7 cells that were grown in a 100 mm dish and proteins equivalent to 15 μl of the lysate were loaded into one lane. Employed antibodies were anti-cofilin antibody, MAB-22 (Abe et al., 1989), anti-P cofilin antibody (Toshima et al., 2001a), anti-His antibody (Qiagen or MBL), anti-phospho-p38 antibody (NEB), or anti-HA antibody, 16B12 (BAbCO). Signals were detected with ECL or ECL plus (Amersham), and band intensity was measured by using Image Gauge (Fuji Film) or Fluor-S MultiImager (BioRad). N-terminal acetylation of cofilin is required for binding of the anti-P cofilin antibody; thus, this antibody does not recognize cofilin that is made in *E. coli* and phosphorylated by LIMK1 in vitro.

Cosedimentation Assay

Purified rabbit muscle actin (Sigma) was polymerized in F buffer (50 mM Tris-HCl [pH 6.8], 100 mM NaCl, 2 mM $MgCl_2$, 1 mM DTT, 0.2 mM ATP, 0.2 mM $CaCl_2$). (Myc+His)-SSH and -hSSHs, expressed in COS-7 cells in a 100 mm dish, were purified by using Ni-NTA agarose, eluted in 15 μl of the imidazole elution buffer, and then centrifuged at 100,000 × g for 10 min to remove aggregates. Cosedimentation assay was performed by addition of 6 μl of SSH eluate to 60 μl of F buffer containing 10 μM F actin and 0.1 mg/ml BSA. After incubation for 60 min at 20°C, the mixture was centrifuged at 100,000 × g for 30 min. The pellet was rinsed once with F buffer. Both supernatant and pellet were dissolved in an equivalent volume of SDS sample buffer and analyzed by 9% SDS-PAGE.

Histological Analyses

Procedures for immunostaining of HeLa cells were essentially as described (Toshima et al., 2001a). *Drosophila* tissues were fixed in 3.7% formaldehyde/PBS at room temperature for 20 min or at 4°C overnight and stained with Alexa 594-conjugated phalliodin (Molecular Probes), purified anti-P cofilin antibody, and/or anti-tag antibodies. Images were collected by using confocal microscopes (BioRad and Zeiss). Adult flies were dehydrated in isoamyl alcohol, dried using a critical point drier, and observed with a scanning electron microscope (SEM) 5800LV (JEOL). Alternatively, flies were quickly frozen in liquid nitrogen and observed with another SEM XL30 (Philips).

Acknowledgments

We thank H. Ando, H. Oda, M. Sone, K. Takeyasu, J.C. Yasuhara, and Y. Nabeshima for allowing R.N. to perform microinjection in their laboratory; S. Ishiguro, N. Matsumoto, K.K. Shimizu, R. Tsugeki, Y. Machida, and K. Okada for use of their scanning electron microscope; and H. Kazama and S. Yohehara for use of their microplate reader. We are also grateful to B.A. Hay, Y. Hiromi, T. Obinata, T. Tabata, the Berkeley Drosophila Genome Project, the Bloomington Stock Center, and the Genetic Stock Research Center at the National Institute of Genetics for reagents. We acknowledge the Human Genome Center at the Institute of Medical Sciences of Tokyo University for use of its databases. Finally, we thank very much M. Adachi, T. Fukuhara, K. Ohashi, T. Tanoue, S.H. Yoshimura, and E. Nishida for technical advice and encouragement. This work was supported by grants to T.U. from Toray Foundation (Japan) for the Promotion of Science and from Core Research for Evolutional Science and Technology. R.N. and K.N.-O. are recipients of a Fellowship of the Japan Society for the Promotion of Science for Junior Scientists.

Received October 12, 2001; revised December 19, 2001.

References

Abe, H., Ohshima, S., and Obinata, T. (1989). A cofilin-like protein is involved in the regulation of actin assembly in developing skeletal muscle. J. Biochem. (Tokyo) *106*, 696–702.

Abe, H., Obinata, T., Minamide, L.S., and Bamburg, J.R. (1996). Xenopus laevis actin-depolymerizing factor/cofilin: a phosphorylation-regulated protein essential for development. J. Cell Biol. *132*, 871–885.

Adams, M.D., Celniker, S.E., Holt, R.A., Evans, C.A., Gocayne, J.D., Amanatides, P.G., Scherer, S.E., Li, P.W., Hoskins, R.A., Galle, R.F., et al. (2000). The genome sequence of *Drosophila melanogaster*. Science *287*, 2185–2195.

Agnew, B.J., Minamide, L.S., and Bamburg, J.R. (1995). Reactivation of phosphorylated actin depolymerizing factor and identification of the regulatory site. J. Biol. Chem. *270*, 17582–17587.

Aizawa, H., Wakatsuki, S., Ishii, A., Moriyama, K., Sasaki, Y., Ohashi, K., Sekine-Aizawa, Y., Sehara-Fujisawa, A., Mizuno, K., Goshima, Y., and Yahara, I. (2001). Phosphorylation of cofilin by LIM-kinase is necessary for semaphorin 3A-induced growth cone collapse. Nat. Neurosci. *4*, 367–373.

Amano, T., Tanabe, K., Eto, T., Narumiya, S., and Mizuno, K. (2001). LIM-kinase 2 induces formation of stress fibres, focal adhesions and membrane blebs, dependent on its activation by Rho-associated kinase-catalysed phosphorylation at threonine-505. Biochem. J. *354*, 149–159.

Ambach, A., Saunus, J., Konstandin, M., Wesselborg, S., Meuer, S.C., and Samstag, Y. (2000). The serine phosphatases PP1 and PP2A associate with and activate the actin-binding protein cofilin in human T lymphocytes. Eur. J. Immunol. *30*, 3422–3431.

Arber, S., Barbayannis, F.A., Hanser, H., Schneider, C., Stanyon, C.A., Bernard, O., and Caroni, P. (1998). Regulation of actin dynamics through phosphorylation of cofilin by LIM-kinase. Nature *393*, 805–809.

Axton, J.M., Dombradi, V., Cohen, P.T., and Glover, D.M. (1990). One of the protein phosphatase 1 isoenzymes in *Drosophila* is essential for mitosis. Cell *63*, 33–46.

Bamburg, J.R. (1999). Proteins of the ADF/cofilin family: essential regulators of actin dynamics. Annu. Rev. Cell Dev. Biol. *15*, 185–230.

Bamburg, J.R., McGough, A., and Ono, S. (1999). Putting a new twist on actin: ADF/cofilins modulate actin dynamics. Trends Cell Biol. *9*, 364–370.

Bartles, J.R. (2000). Parallel actin bundles and their multiple actin-bundling proteins. Curr. Opin. Cell Biol. *12*, 72–78.

Baum, B., and Perrimon, N. (2001). Spatial control of the actin cytoskeleton in *Drosophila* epithelial cells. Nat. Cell Biol. *3*, 883–890.

Baum, B., Li, W., and Perrimon, N. (2000). A cyclase-associated protein regulates actin and cell polarity during Drosophila oogenesis and in yeast. Curr. Biol. *10*, 964–973.

Benlali, A., Draskovic, I., Hazelett, D.J., and Treisman, J.E. (2000). *act up* controls actin polymerization to alter cell shape and restrict Hedgehog signaling in the Drosophila eye disc. Cell *101*, 271–281.

Borisy, G.G., and Svitkina, T.M. (2000). Actin machinery: pushing the envelope. Curr. Opin. Cell Biol. *12*, 104–112.

Brand, A.H., and Perrimon, N. (1993). Targeted gene expression as a means of altering cell fates and generating dominant phenotypes. Development *118*, 401–415.

Carlier, M.F., Laurent, V., Santolini, J., Melki, R., Didry, D., Xia, G.X., Hong, Y., Chua, N.H., and Pantaloni, D. (1997). Actin depolymerizing factor (ADF/cofilin) enhances the rate of filament turnover: implication in actin-based motility. J. Cell Biol. *136*, 1307–1322.

Chen, H., Bernstein, B.W., and Bamburg, J.R. (2000). Regulating actin-filament dynamics in vivo. Trends Biochem. Sci. *25*, 19–23.

Chen, J., Godt, D., Gunsalus, K., Kiss, I., Goldberg, M., and Laski, F.A. (2001). Cofilin/ADF is required for cell motility during *Drosophila* ovary development and oogenesis. Nat. Cell Biol. *3*, 204–209.

Cohen, P. (1990). The structure and regulation of protein phosphatases. Adv. Second Messenger Phosphoprotein Res. *24*, 230–235.

Cong, J., Geng, W., He, B., Liu, J., Charlton, J., and Adler, P.N. (2001). The *furry* gene of *Drosophila* is important for maintaining the integrity of cellular extensions during morphogenesis. Development *128*, 2793–2802.

Cooley, L., Verheyen, E., and Ayers, K. (1992). *chickadee* encodes a profilin required for intercellular cytoplasm transport during *Drosophila* oogenesis. Cell *69*, 173–184.

DeRosier, D.J., and Tilney, L.G. (2000). F-actin bundles are derivatives of microvilli: what does this tell us about how bundles might form? J. Cell Biol. *148*, 1–6.

Edwards, K.A., Montague, R.A., Shepard, S., Edgar, B.A., Erikson, R.L., and Kiehart, D.P. (1994). Identification of *Drosophila* cytoskeletal proteins by induction of abnormal cell shape in fission yeast. Proc. Natl. Acad. Sci. USA *91*, 4589–4593.

Geng, W., He, B., Wang, M., and Adler, P.N. (2000). The *tricornered* gene, which is required for the integrity of epidermal cell extensions, encodes the *Drosophila* nuclear DBF2-related kinase. Genetics *156*, 1817–1828.

Guan, K.L., Broyles, S.S., and Dixon, J.E. (1991). A Tyr/Ser protein phosphatase encoded by vaccinia virus. Nature *350*, 359–362.

Gunsalus, K.C., Bonaccorsi, S., Williams, E., Verni, F., Gatti, M., and Goldberg, M.L. (1995). Mutations in *twinstar*, a *Drosophila* gene encoding a cofilin/ADF homologue, result in defects in centrosome migration and cytokinesis. J. Cell Biol. *131*, 1243–1259.

Hay, B.A., Wolff, T., and Rubin, G.M. (1994). Expression of baculovirus P35 prevents cell death in *Drosophila*. Development *120*, 2121–2129.

He, B., and Adler, P.N. (2001). Cellular mechanisms in the development of the *Drosophila* arista. Mech. Dev. *104*, 69–78.

Hopmann, R., Cooper, J.A., and Miller, K.G. (1996). Actin organization, bristle morphology, and viability are affected by actin capping protein mutations in *Drosophila*. J. Cell Biol. *133*, 1293–1305.

Jiang, J., and Struhl, G. (1998). Regulation of the Hedgehog and Wingless signalling pathways by the F-box/WD40-repeat protein Slimb. Nature *391*, 493–496.

Kennerdell, J.R., and Carthew, R.W. (2000). Heritable gene silencing in *Drosophila* using double-stranded RNA. Nat. Biotechnol. *18*, 896–898.

Keyse, S.M. (1995). An emerging family of dual specificity MAP kinase phosphatases. Biochim. Biophys. Acta *1265*, 152–160.

Klaes, A., Menne, T., Stollewerk, A., Scholz, H., and Klambt, C. (1994). The Ets transcription factors encoded by the *Drosophila* gene *pointed* direct glial cell differentiation in the embryonic CNS. Cell *78*, 149–160.

Lu, B., Usui, T., Uemura, T., Jan, L., and Jan, Y.N. (1999). Flamingo controls the planar polarity of sensory bristles and asymmetric division of sensory organ precursors in Drosophila. Curr. Biol. *9*, 1247–1250.

Maekawa, M., Ishizaki, T., Boku, S., Watanabe, N., Fujita, A., Iwamatsu, A., Obinata, T., Ohashi, K., Mizuno, K., and Narumiya, S. (1999). Signaling from Rho to the actin cytoskeleton through protein kinases ROCK and LIM-kinase. Science *285*, 895–898.

Meberg, P.J., Ono, S., Minamide, L.S., Takahashi, M., and Bamburg, J.R. (1998). Actin depolymerizing factor and cofilin phosphorylation dynamics: response to signals that regulate neurite extension. Cell Motil. Cytoskeleton *39*, 172–190.

Mitchell, H.K., Edens, J., and Petersen, N.S. (1990). Stages of cell hair construction in *Drosophila*. Dev. Genet. *11*, 133–140.

Moon, A., and Drubin, D.G. (1995). The ADF/cofilin proteins: stimulus-responsive modulators of actin dynamics. Mol. Biol. Cell *6*, 1423–1431.

Moriyama, K., Iida, K., and Yahara, I. (1996). Phosphorylation of Ser-3 of cofilin regulates its essential function on actin. Genes Cells *1*, 73–86.

Nagaoka, R., Abe, H., Kusano, K., and Obinata, T. (1995). Concentration of cofilin, a small actin-binding protein, at the cleavage furrow during cytokinesis. Cell Motil. Cytoskeleton *30*, 1–7.

Newsome, T.P., Asling, B., and Dickson, B.J. (2000). Analysis of *Drosophila* photoreceptor axon guidance in eye-specific mosaics. Development *127*, 851–860.

Ohashi, K., Hosoya, T., Takahashi, K., Hing, H., and Mizuno, K. (2000a). A *Drosophila* homolog of LIM-kinase phosphorylates cofilin and induces actin cytoskeletal reorganization. Biochem. Biophys. Res. Commun. *276*, 1178–1185.

Ohashi, K., Nagata, K., Maekawa, M., Ishizaki, T., Narumiya, S., and Mizuno, K. (2000b). Rho-associated kinase ROCK activates LIM-kinase 1 by phosphorylation at threonine 508 within the activation loop. J. Biol. Chem. *275*, 3577–3582.

Overton, J. (1967). The fine structure of developing bristles in wild type and mutant *Drosophila melanogaster*. J. Morphol. *122*, 367–379.

Pollard, T.D., Blanchoin, L., and Mullins, R.D. (2000). Molecular

mechanisms controlling actin filament dynamics in nonmuscle cells. Annu. Rev. Biophys. Biomol. Struct. *29*, 545–576.

Robertson, H.M., Preston, C.R., Phillis, R.W., Johnson-Schlitz, D.M., Benz, W.K., and Engels, W.R. (1988). A stable genomic source of P element transposase in *Drosophila melanogaster*. Genetics *118*, 461–470.

Rubin, G.M., Hong, L., Brokstein, P., Evans-Holm, M., Frise, E., Stapleton, M., and Harvey, D.A. (2000). A *Drosophila* complementary DNA resource. Science *287*, 2222–2224.

Spradling, A.C., Stern, D.M., Kiss, I., Roote, J., Laverty, T., and Rubin, G.M. (1995). Gene disruptions using P transposable elements: an integral component of the *Drosophila* genome project. Proc. Natl. Acad. Sci. USA *92*, 10824–10830.

Spradling, A.C., Stern, D., Beaton, A., Rhem, E.J., Laverty, T., Mozden, N., Misra, S., and Rubin, G.M. (1999). The Berkeley *Drosophila* Genome Project gene disruption project: single P-element insertions mutating 25% of vital *Drosophila* genes. Genetics *153*, 135–177.

Streuli, M., Krueger, N.X., Tsai, A.Y., and Saito, H. (1989). A family of receptor-linked protein tyrosine phosphatases in humans and *Drosophila*. Proc. Natl. Acad. Sci. USA *86*, 8698–8702.

Sumi, T., Matsumoto, K., Takai, Y., and Nakamura, T. (1999). Cofilin phosphorylation and actin cytoskeletal dynamics regulated by rho- and Cdc42-activated LIM-kinase *2*. J. Cell Biol. *147*, 1519–1532.

Sutherland, J.D., and Witke, W. (1999). Molecular genetic approaches to understanding the actin cytoskeleton. Curr. Opin. Cell Biol. *11*, 142–151.

Tanoue, T., Moriguchi, T., and Nishida, E. (1999). Molecular cloning and characterization of a novel dual specificity phosphatase, MKP-5. J. Biol. Chem. *274*, 19949–19956.

Theriot, J.A. (1997). Accelerating on a treadmill: ADF/cofilin promotes rapid actin filament turnover in the dynamic cytoskeleton. J. Cell Biol. *136*, 1165–1168.

Tilney, L.G., Tilney, M.S., and Guild, G.M. (1995). F actin bundles in *Drosophila* bristles. I. Two filament cross-links are involved in bundling. J. Cell Biol. *130*, 629–638.

Tilney, L.G., Connelly, P., Smith, S., and Guild, G.M. (1996). F-actin bundles in *Drosophila* bristles are assembled from modules composed of short filaments. J. Cell Biol. *135*, 1291–1308.

Tilney, L.G., Connelly, P.S., Vranich, K.A., Shaw, M.K., and Guild, G.M. (2000). Actin filaments and microtubules play different roles during bristle elongation in *Drosophila*. J. Cell Sci. *113*, 1255–1265.

Toshima, J., Tanaka, T., and Mizuno, K. (1999). Dual specificity protein kinase activity of testis-specific protein kinase 1 and its regulation by autophosphorylation of serine-215 within the activation loop. J. Biol. Chem. *274*, 12171–12176.

Toshima, J., Toshima, J.Y., Amano, T., Yang, N., Narumiya, S., and Mizuno, K. (2001a). Cofilin phosphorylation by protein kinase testicular protein kinase 1 and its role in integrin-mediated actin reorganization and focal adhesion formation. Mol. Biol. Cell *12*, 1131–1145.

Toshima, J., Toshima, J.Y., Takeuchi, K., Mori, R., and Mizuno, K. (2001b). Cofilin phosphorylation and actin reorganization activities of testicular protein kinase 2 and its predominant expression in testicular Sertoli cells. J. Biol. Chem. *276*, 31449–31458.

Toshima, J.Y., Toshima, J., Watanabe, T., and Mizuno, K. (2001c). Binding of 14-3-3beta regulates the kinase activity and subcellular localization of testicular protein kinase 1. J. Biol. Chem. *276*, 43471–43481.

Usui, T., Shima, Y., Shimada, Y., Hirano, S., Burgess, R.W., Schwarz, T.L., Takeichi, M., and Uemura, T. (1999). Flamingo, a seven-pass transmembrane cadherin, regulates planar cell polarity under the control of Frizzled. Cell *98*, 585–595.

Verheyen, E.M., and Cooley, L. (1994). Profilin mutations disrupt multiple actin-dependent processes during *Drosophila* development. Development *120*, 717–728.

Wassarman, D.A., Solomon, N.M., Chang, H.C., Karim, F.D., Therrien, M., and Rubin, G.M. (1996). Protein phosphatase 2A positively and negatively regulates Ras1-mediated photoreceptor development in *Drosophila*. Genes Dev. *10*, 272–278.

Welch, M.D., Mallavarapu, A., Rosenblatt, J., and Mitchison, T.J. (1997). Actin dynamics in vivo. Curr. Opin. Cell Biol. *9*, 54–61.

Wodarz, A., Hinz, U., Engelbert, M., and Knust, E. (1995). Expression of *crumbs* confers apical character on plasma membrane domains of ectodermal epithelia of *Drosophila*. Cell *82*, 67–76.

Xu, T., and Rubin, G.M. (1993). Analysis of genetic mosaics in developing and adult *Drosophila* tissues. Development *117*, 1223–1237.

Yahara, I., Aizawa, H., Moriyama, K., Iida, K., Yonezawa, N., Nishida, E., Hatanaka, H., and Inagaki, F. (1996). A role of cofilin/destrin in reorganization of actin cytoskeleton in response to stresses and cell stimuli. Cell Struct. Funct. *21*, 421–424.

Yang, N., Higuchi, O., Ohashi, K., Nagata, K., Wada, A., Kangawa, K., Nishida, E., and Mizuno, K. (1998). Cofilin phosphorylation by LIM-kinase 1 and its role in Rac-mediated actin reorganization. Nature *393*, 809–812.